



Asian Journal of Chemistry; Vol. 26, No. 16 (2014), 4952-4958

ASIAN JOURNAL OF CHEMISTRY

<http://dx.doi.org/10.14233/ajchem.2014.16265>



Fabrication and Characterization of ZnO/MWCNTs with Enhanced Photocatalytic Activity

ABDULLAH H. QUSTI

Chemistry Department, Faculty of Science, King Abdulaziz University, P.O Box 80200, Jeddah 21589, Kingdom of Saudi Arabia

Corresponding author: Fax: +966 2 6952292; Tel: +966 50811447; Email: profaqusti@outlook.com

Received: 31 August 2013;

Accepted: 22 October 2013;

Published online: 28 July 2014;

AJC-15608

Composite of multi-walled carbon nanotubes (MWCNTs) and zinc oxide (ZnO) were prepared by the sol-gel method. The photocatalytic function of the MWCNTs/ZnO was validated for cyanide degradation as a model of organic pollutant under irradiation of visible light. The catalysts were characterized by X-ray diffraction, specific surface area measurement, energy dispersive X-ray spectrum analysis, transmission electron microscopy and UV-visible absorption spectra. The results show that the ZnO/ MWCNTs composites (4 % mass ratio of MWCNTs) exhibits much higher photocatalytic activity than other ratios and in addition higher than that of TiO₂ (P-25). The promotion is mainly contributed from electron transfer between ZnO and MWCNT.

Keywords: Sol-gel; Zinc oxide/multi-walled carbon nanotubes, Composite, Photocatalyst.

INTRODUCTION

Environmental problems, especially, the sustained pollutions of air and water by various organic and metallic ion contaminants receive extensive attentions. Many efforts are dedicated to the remediation of environmental pollution. For instance, photodegradation of organic compounds provides an available way for remediation of water pollution¹⁻⁴. Nanostructured semiconductors are proved to be an excellent photocatalyst which can degrade most kinds of persistent organic pollution.

Photocatalytic technology has attracted extensive attention for its cleaning, no second pollution and deep oxidation-reduction reaction under ambient temperature. A number of research topics in photocatalysis have emerged and offered the potentials for commercial development and environmental protection, such as splitting water to produce hydrogen fuel^{5,6}, selective synthesis of organic compounds⁷, removal of organic or inorganic pollutants^{8,9}, solar cells and sensors¹⁰. In addition to TiO₂, other binary metal oxides have been studied to determine their photocatalytic oxidation properties. Zinc oxide has been often considered a valid alternative to TiO₂¹¹, because of its good optoelectronic, catalytic and photochemical properties along with its low cost. Zinc oxide has a band gap of 3.3 eV that is lower than that of anatase. Due to the position of the valence band of ZnO, the photogenerated holes have strong enough oxidizing power to decompose most organic compounds¹². Zinc oxide has been tested to decompose aqueous solutions of several dyes¹³⁻³² and many other environmental pollutants³³⁻⁴⁵. Several studies have shown that ZnO is quite

active under visible light illumination for the photodegradation of some organic compounds in aqueous solution^{18-21,40}.

Since being reported in 1991, carbon nanotubes have received much interest for their unique electrical property and large specific surface area and hence been used as a representative system for the study of electronic transport at the nano-scale^{46,47}. The physical properties of high mechanical strength and large specific surface area, hollow and layered structures of carbon nanotubes make carbon nanotubes to be a good supporting material for catalysts. In addition, carbon nanotubes show higher electron conducting ability and higher adsorption capacity, which means they can act as promising materials in environmental cleaning. Combining the efficient photocatalytic activity of ZnO with the excellent adsorption and charge transfer abilities of carbon nanotubes, the composites of titania and carbon nanotubes have been considered as more advanced candidate of photocatalyst. Various different structural forms of titania-carbon nanotubes photocatalysts have been prepared, such as ZnO nanoparticles on MWCNTs, it shows noticeable performances because of the excellent electron conducting properties of MWCNT. Multi-walled carbon nanotube is an excellent one-dimension supporter. It has shown unique superiority when it is decorated with metal particles and metal oxides⁴⁸⁻⁵¹. Furthermore, MWCNT could be considered as a good electron acceptor for its unique structure⁵². Owing the unique features, it can serve as a good template of photocatalyst. The photoexcited electron will transfer from semiconductors to MWCNT when the photocatalytic semiconducting oxides are coated on MWCNT. The transfer prohibits the

recombination rates of electron-hole pairs. This offers a feasible way to improve the photocatalytic efficiency. The previous studies indicated that some semiconductors-MWCNT composites exhibited enormous application perspective in photocatalysis^{53,54}.

In this study, MWCNT/ZnO nano-composites were synthesized *via* acid-catalyzed sol-gel method, the characterization the resulting composite explained under experimental section in details. This work has been motivated by potential application of ZnO/MWCNT nano-composite as a novel photo-active material for cyanide removal under visible-irradiation. Furthermore, compared to the present work; (ZnO, P₂₅ and MWCNT) were employed within the photodegradation test.

EXPERIMENTAL

High purity MWCNT was purchased then used in the procedure as received, (Sigma-Aldrich Co., Ltd., USA). Zinc diethyl Zn (C₂H₅)₂ (52 %, Aldrich) and Nitric acid (65 %) were used. All the reagents were used as received. All aqueous solutions were prepared using doubly distilled water.

Synthesis of MWCNT/ZnO: MWCNT-ZnO was synthesized using a modified acid-catalyzed sol-gel method. In typical method, 0.1 mol of Zn (OC₂H₅)₂ was dissolved in 200 mL of ethanol, then the solution was stirring in ambient temperature for 0.5 h, this is followed by adding 1.56 mL of nitric acid, the resulted solution mixture labeled (A).

Subsequently, as a second step a certain amount of MWCNT was introduced into the previous solution mixture (A), then; covered and kept stirring until a homogenous MWCNT contained gel formed. The gel was left in air for several days and then the obtained xerogel was crushed into a fine powder. The powder was calcined at 400 °C in a flow of N₂ for 2 h in order to obtain MWCNT/ZnO composite materials. MWCNTs and ZnO were dispersed in the solution with different MWCNTs: ZnO mass ratios of 0:1, 1:1, 2:1, 3:1, 4:1, 5:1; named after ZnO, 1 MWCNT-ZnO, 2 MWCNT-ZnO, 3 MWCNT-ZnO, 4 MWCNT-ZnO and 5 MWCNT-ZnO respectively.

Characterization techniques: Different techniques were applied for the characterization of MWCNT/ZnO nanocomposite. X-ray diffraction (XRD) (Philips X pert pro) was employed to determine crystalline phases and average crystalline size. Energy dispersive X-ray (EDX) and microscopic structures were investigated with a JEM 2100 transmission electron microscope (TEM) to analyze the surface chemical composition of the prepared catalyst. The Brunauer-Emmet-Teller (BET) surface area of the MWCNT/ZnO was evaluated from the N₂-absorption-desorption isotherms at 77 k were measured using a Nova 2000 series apparatus (Chromatech) and the surface area was calculated according to the corresponding BET equation. UV-visible spectrometer (Perkin Elmer Lambda 950) was used to record the UV-visible absorption spectra.

Photocatalytic degradation: Application of synthesized nanocomposite for the photodegradation of cyanide was investigated under visible light. The experiments were carried out using a horizontal cylinder annular batch reactor. The photocatalyst was irradiated with a blue fluorescent lamp (150 W, maximum energy at 450 nm) doubly covered with a

UV cut filter. The intensity data of UV light is confirmed to be under the detection limit (0.1 mW/cm²) of a UV radiometer. In a typical experiment, 0.0166 wt. % of calcined ZnO/MWCNTs, ZnO and TiO₂ degussa P₂₅ were dissolved into a 300 mL, 100 mg/L potassium cyanide (KCN) solution (pH = 8.5), which was adjusted by ammonia solution. The reaction was carried out isothermally at 25 °C and samples of the reaction mixture were taken at different intervals for a total reaction time of one hour. The CN⁻_(aq) concentration in the samples was estimated by volumetric titration with AgNO₃, using potassium iodide to determine the titration end-point⁵⁵. The removal efficiency of CN⁻_(aq) has been measured by applying the following equation:

$$\% \text{ Removal efficiency} = (C_0 - C)/C_0 \times 100$$

where C₀ is the initial concentration of uncomplexed CN⁻_(aq) in solution and C is the concentration of unoxidized CN⁻_(aq) in solution.

RESULTS AND DISCUSSION

X-ray diffraction (XRD) analysis was carried out to detect the presence of various species. Fig. 1 presents the XRD spectra of pristine MWCNT, ZnO and MWCNT/ZnO.

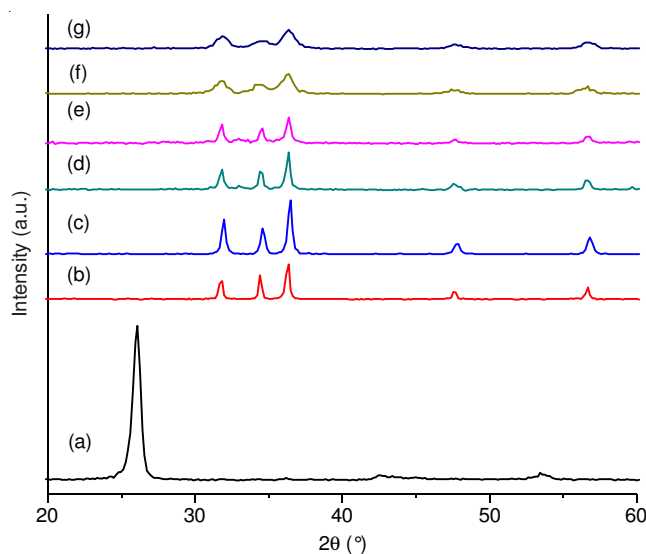


Fig. 1. X-ray diffraction patterns of (a) MWCNT, (b) ZnO, (c) 1-MWCNT-ZnO, (d) 2-MWCNT-ZnO, (e) 3-MWCNT-ZnO, (f) 4-MWCNT-ZnO and (g) 5-MWCNT-ZnO

A deep look reveals that, in case of the MWCNT/ZnO composites; it is difficult to elicit the characteristic peak of MWCNT from the spectrum of the composites because of the good crystallization of ZnO and their fine attachment on to MWCNT. It is noteworthy that only ZnO phase appeared in the spectra pertaining to both ZnO and MWCNT/ZnO composites which means that, the structure of ZnO in the composites is almost the same. This indicates that there is no difference in the microstructure of ZnO before and after combination with MWCNT. The width of the reflections is considerably broadened with increase of the weight ration of MWCNT for the composites, indicating a small crystalline domain size, which can be roughly quantified by Scherrer's

equation. According to Debye-Scherrer formula, the average crystallite size of neat ZnO is 57.6 nm while this size is decreasing to 12.3 nm with the attachment of ZnO to MWCNT in ZnO/MWCNT composites and the same observation detected with all molar ratios as tabulated in Table-1. Because the size of ZnO is about 57 nm and size of MWCNT is about 22 nm, therefore addition of high wt % of MWCNT will decrease the size of ZnO and made the peak more broad and consequently, the size will be decreased.

Sample	BET ($\text{m}^2 \text{g}^{-1}$)	d (nm)
ZnO	75	57.6
1-MWCNT- ZnO	80	42.6
2-MWCNT- ZnO	85	33.2
3-MWCNT- ZnO	97	14.1
4-MWCNT- ZnO	108	12.3
5-MWCNT- ZnO	155	10.6
MWCNTs	150	21.7

Energy dispersive X-ray (EDX) spectrum analysis of MWCNT/ZnO samples Fig. 2 clearly reveals the presence of C, O and Zn elements, also indicating the actual deposition of ZnO on MWCNT. The spectra of other composite catalysts indicate different intensity of peaks assigned to C due to different MWCNT content.

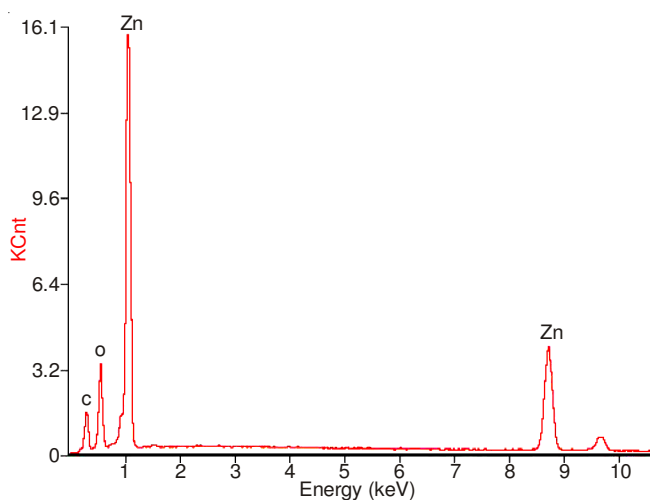


Fig. 2. EDX spectrum of 4-MWCNT-ZnO

Morphology study of (ZnO, MWCNTs and ZnO/MWCNTs): The BET surface area of ZnO, MWCNTs and MWCNT/ZnO composites with different molar ratios are tabulated in Table-1. The surface area of ZnO and MWCNT are 75 and 150 m^2/g , respectively. The BET surface area of MWCNTs/ZnO composites vary from 80 to 156 m^2/g , increasing with increasing MWCNTs content in the composites. This can be explained by the fact that MWCNTs have a high surface area and the combination of MWCNTs with ZnO can increase the surface area of ZnO in the composites. This suggests that MWCNTs has a significant effect on the adsorption ability of ZnO. All the adsorption-desorption isotherms obey type IV; which confirm that a mesoporous pore texture of the nanotubes

can be preserved after the introduction of ZnO. Fig. 3 illustrates the adsorption-desorption isotherm pertaining to MWCNT/ZnO (1:4) mass ratio. The isotherm of MWCNT is identical with the reported ones, where pores in MWCNT can be mainly divided into inner hollow cavities of small diameter and aggregated pores formed by interaction of isolated MWCNT⁵⁶.

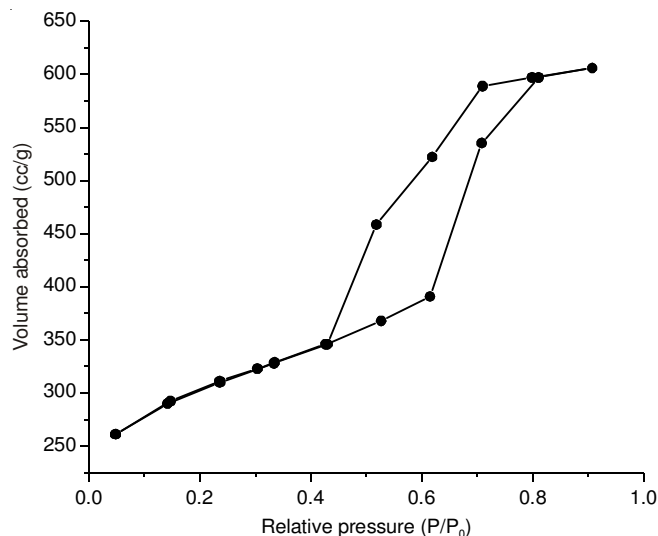


Fig. 3. N_2 -adsorption -desorption isotherm of 4-MWCNT-ZnO

Direct evidence of the formation of ZnO nanoparticles on the MWCNT surface is given by TEM images. Fig. 4 presents TEM micrographs of MWCNT/ZnO with different mass ratios. The images reveal that the MWCNTs come in contact with one another and embedded the ZnO nanoparticles as presented in Fig. 4a. On the other side, Fig. 4b illustrates uniformly dispersion and coverage of all ZnO nanoparticles on MWCNT surface, which is observed more explicitly with high magnification which indicates again that MWCNTs were all well dispersed on the surface of the ZnO particles and that the MWCNTs and ZnO particles were in close contact with each other. The average particle size of ZnO determined from the TEM images is about 7.5 nm, which is consistent with XRD results.

UV-visible spectroscopy: The diffuse reflectance UV-visible spectra of different solid catalysts, where Kubelka-Munk equivalent absorption units are used, are displayed in Fig. 5.

The synthesized MWCNTs showed a shift of the absorption edge towards higher wavelengths (red shift) which corresponds with a decrease in the band gap energy. Besides, the synthesized ZnO has no shift of its sharp fundamental absorption edge which located at 400 nm. The band gap energies (E_g) calculated on the basis of the corresponding absorption edges are shown in Table-2. It can be seen from Table-2 that the absorption edge of the MWCNT/ZnO, or the band gap energy, changed with the MWCNT percent. The band gap energy of the coupled MWCNT/ZnO photocatalyst decreased with the increasing the MWCNT per cent.

Moreover, the composite catalyst ZnO/MWCNT absorbs at wavelengths higher than that of ZnO, which constitutes an advantage considering sun light harnessing and increases with MWCNT content^{57,58}, where; an apparent enhancement of

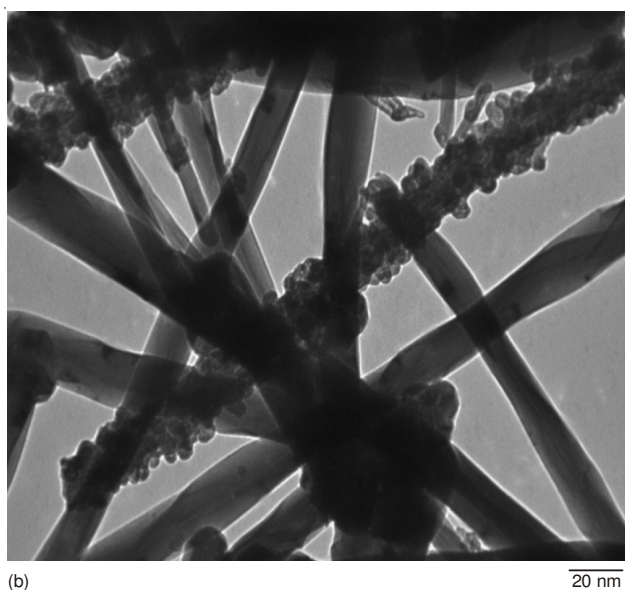
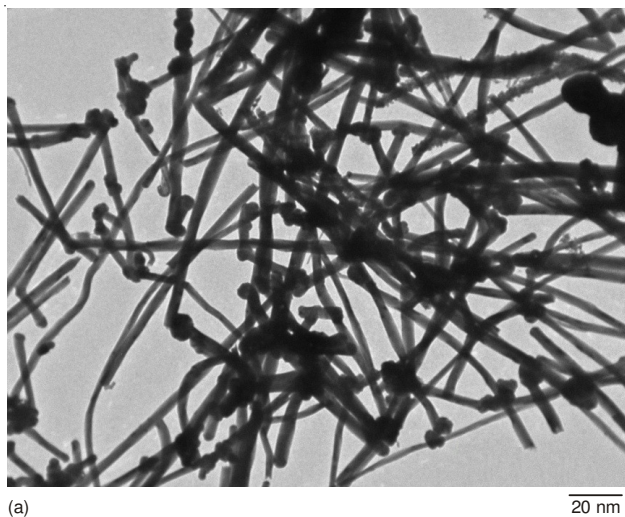


Fig. 4. TEM images of 4-MWCNT-ZnO; (a) overall view of MWCNT embedding in ZnO matrix and in inset MWCNT surface covered with ZnO nanoparticles; (b) ZnO nanoparticle on MWCNT surface with a higher magnification

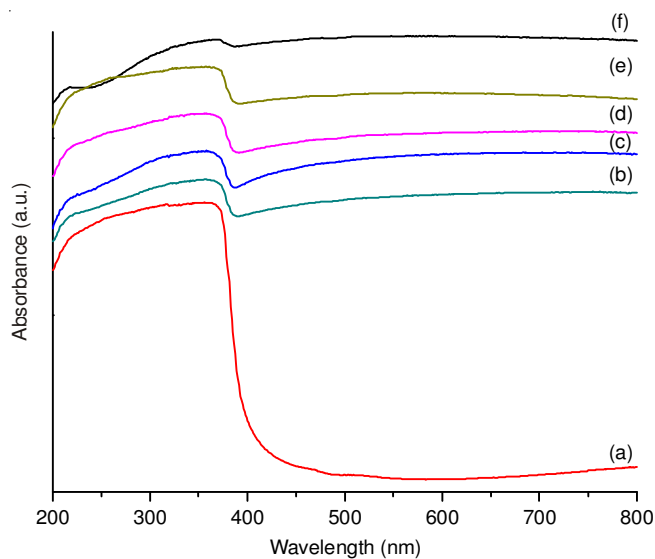


Fig. 5. UV-visible spectra of (a) ZnO, (b) 1-MWCNT-ZnO, (c) 2-MWCNT-ZnO, (d) 3-MWCNT-ZnO, (e) 4-MWCNT-ZnO, (f) 5-MWCNT-ZnO

Sample	Band gap energy, eV
MWCNT	—
ZnO	3.10
1 % MWCNT/ZnO	2.97
2 % MWCNT/ZnO	2.90
3 % MWCNT/ZnO	2.89
4 % MWCNT/ZnO	2.75
5 % MWCNT/ZnO	2.70

absorption is observed even for the composite catalyst with 1 % MWCNT content, then the absorption is totally over the whole range of the UV-visible spectrum for 5 % MWCNT content and this a clear meaning on the relation between absorption and MWCNT content. These observations may indicate an increment of surface electric charge of the oxides in composite catalysts (ZnO/MWCNTs) due to the introduction of MWCNT.

Photocatalytic performance

Effect of deposition amount of MWCNTs on ZnO activity:

As shown in Fig. 6, the photocatalytic activity decreases gradually as the amount of MWCNTs present in the composites decreases. This behavior may be attributed to the positive effect of MWCNTs. Since it can conduct electrons⁵⁹, so it has the ability to avoid recombination of electron/hole pairs. In addition to the photo-induced electrons in MWCNTs may trigger the formation of radicals in ZnO (superoxide radical ion and/or hydroxyl radical), which are responsible for the degradation of the organic compound⁶⁰⁻⁶². The observation suggests that the high amount of MWCNTs inhibits the photocatalytic activity of ZnO, because of the color of MWCNTs is black which can shield the light absorption by ZnO. If there is no light absorption for ZnO, the samples cannot show any photocatalytic activity therefore the photocatalytic effect decreases.

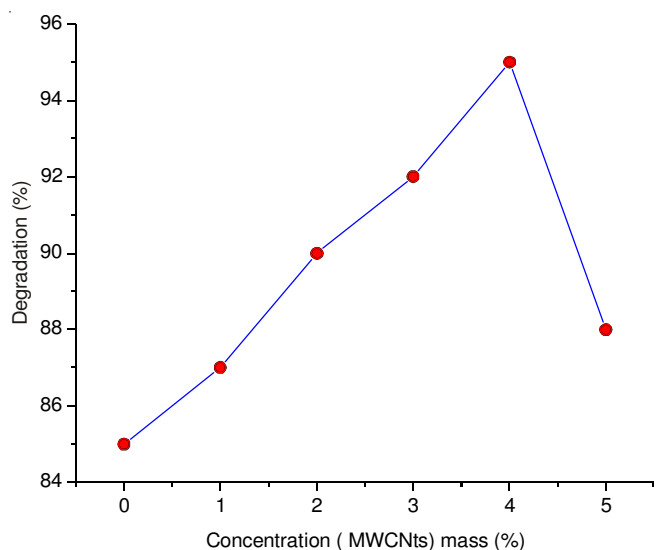


Fig. 6. Relation between cyanide degradation % and MWCNTs content

Effect of different catalyst on photocatalytic degradation of cyanide:

Fig. 7 compares the photocatalytic degradation

of cyanide in the presence of the neat ZnO powder, TiO₂ degussa P₂₅, MWCNTs and ZnO/MWCNTs composites under irradiation of UV-visible light. It is obvious that ZnO/MWCNTs nanocomposites 4 % present a high photocatalytic activity compared to the neat ZnO powder and P₂₅. This behavior may be attributed to: (1) MWCNTs can conduct electron and reduce electronic accumulation of ZnO, they can decrease the recombination of electron/hole pairs. At the same time, MWCNTs without highly tangled structure can be suspended, sorted and manipulated more easily, hence the light can well penetrate into the inner tubes. (2) Their large specific surface area, hollow and layered structures indicate that they can adsorb the cyanide substance of solutions, centralize on the surface of ZnO and also favor the photocatalytic activity. (3) Because of the lights only penetrate the outer surface of nanoparticles about 1-2 nm, when the catalyst is pure ZnO nanoparticles, the effect of utilization is only confined to the outer surface. Once it compounds with MWCNTs, because MWCNTs are open at both ends, the light will enter into the inner space of MWCNTs, the composite will form two depletion layers⁶³-one is on the outer surface of the ZnO nanoparticles and the other is at the interface between MWCNTs and ZnO and thus the activity of catalyst can be strongly strengthened.

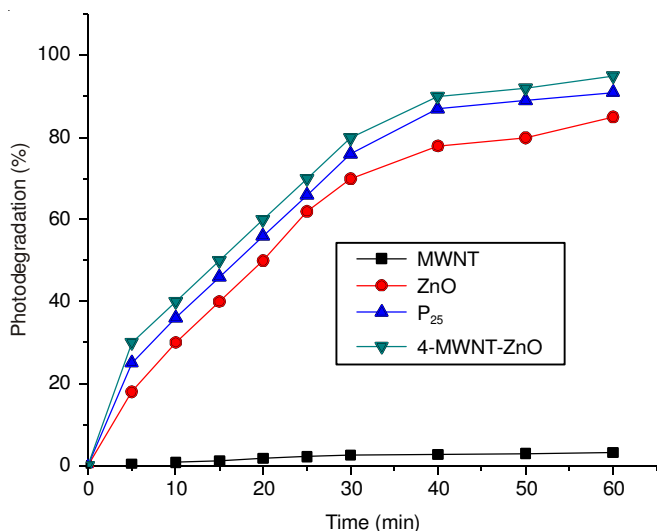


Fig. 7. Effect of different catalysts on photocatalytic degradation %

Kinetics study of reaction: To obtain a quantitative understanding on the reaction kinetics of the cyanide degradation, we apply the pseudo-first order model⁶⁴ as expressed by equation $\text{Log } C_t = -kt + \text{Log } C_0$, which is generally used for photodegradation if the initial concentration of the pollutant is low⁶⁵. Where C_0 and C_t represent the concentration of the substrate in solution at zero time and t time of illumination, respectively and k represents the apparent rate constant (min^{-1}).

Fig. 8 depicts the photocatalytic reaction kinetics of cyanide degradation in solution. The apparent rate constants are summarized in Table-3. The reaction constant k is $0.003: 0.0223 \text{ min}^{-1}$, indicating that the 4 % MWCNT/ZnO composites have a great photocatalytic activity towards the photodegradation of cyanide. As mentioned above, MWCNT /ZnO composites are rich in surface hydroxyl groups. Furthermore, electronic interaction between the surface ZnO and MWCNT substrate could occur

for composites. The abundant hydroxyl groups adsorbed on the surface of composites can lead to the formation of considerable hydroxyl radicals, which oxidizes the adsorbed cyanide on the surface⁶⁶.

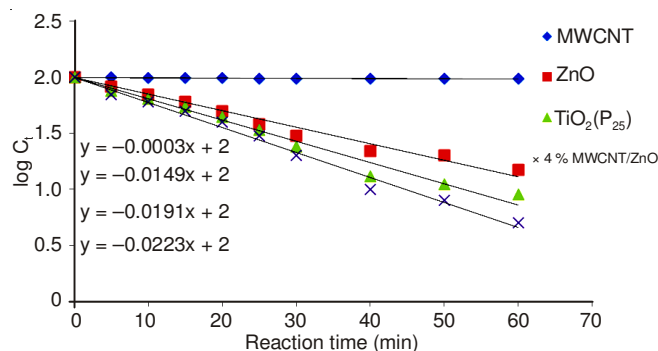
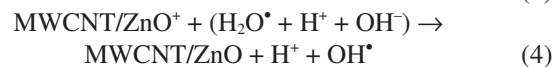


Fig. 8. Rate constant of reaction kinetic of cyanide with different catalyst types

TABLE-3	
RATE CONSTANT VALUES OF CYANIDE REACTION KINETIC	
Sample	$k \times 10^{-4} (\text{min}^{-1})$
MWCNT	3
ZnO	149
TiO ₂ (P ₂₅)	191
4 % MWCNT/ZnO	223

Fig. 9 shows the schematic mechanism of the photocatalysis by MWCNT/ZnO composites when MWCNT introduced. Considering the semiconductive properties of carbon nanotubes, MWCNTs might accept the photo-induced electron (e^-) into the conduction band of the ZnO particles by visible irradiation (Eqn. 1). It is considered that the electrons in MWCNTs are transferred to the conduction band in the ZnO particles. In this time, the electrons in conduction band might react with O₂, which can trigger the formation of very reactive superoxide radical ion (O₂^{•-}). Simultaneously, a positive charged hole (h⁺) might be formed with electron transfer from valence bond in ZnO to MWCNTs (eqn. 3). The positive charged hole (h⁺) might react with the OH⁻ derived from H₂O. With this understanding, the role played by MWCNTs can be illustrated by injecting electrons into ZnO conduction band under visible irradiation and triggering the formation of very reactive superoxide radical ion O₂^{•-} (eqn. 2) and hydroxyl radical OH[•] (eqn. 4). Consequently, both radical groups (superoxide radical ion O₂^{•-} and hydroxyl radical OH[•]) are responsible for the degradation of the organic compound. The as-suggested electron transfer between carbon and ZnO was experimentally supported by our early investigation.



Conclusion

An easy approach to prepare a recoverable and effective photocatalyst with a uniform microstructure of MWCNTs/ZnO composite was proposed. In this approach MWCNTs/ZnO have been prepared by the sol-gel method.

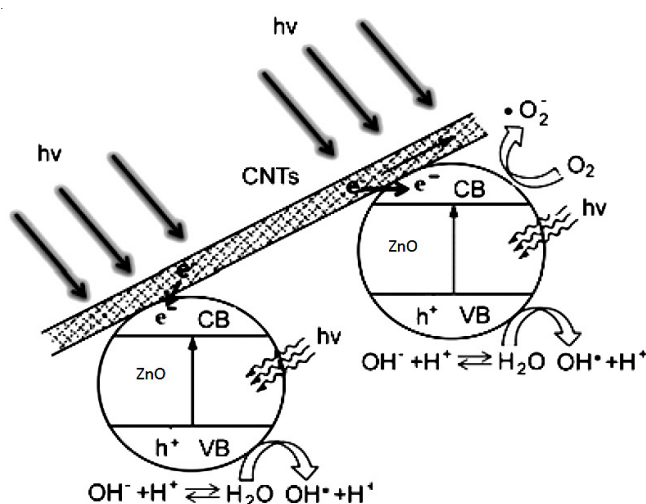


Fig. 9. Mechanism for the CNT/ZnO composites

The morphology of MWCNTs covered with ZnO was carried out by HRTEM images. The size of ZnO nanoparticles on the surface of the MWCNTs revealed by XRD measurements approved by HRTEM. The microstructure of ZnO before combination with MWCNTs is similar with that of ZnO after combination with MWCNTs. The addition of MWCNTs to the composites improved the photocatalysis of ZnO. The MWCNTs/ZnO composite was evaluated on the basis of the degradation of model compounds such as cyanide (one of the organic pollutants).

The presence of a small amount of MWCNTs can enhance photocatalytic activity of ZnO greatly; this success is attributed to the synergistic effect of ZnO and MWCNTs in the MWCNTs/ZnO composite during the photo-catalytic reaction. The MWCNTs/ZnO composite is an effective photo-catalyst for the removal of cyanide from waste water.

REFERENCES

- K. Rajeshwar and N.R. de Tacconi, *Chem. Soc. Rev.*, **38**, 1984 (2009).
- C.A. Martinez-Huitle and E. Brillias, *Appl. Catal. B*, **87**, 105 (2009).
- X.W. Zhang, T. Zhang, J. Ng and D.D. Sun, *Adv. Funct. Mater.*, **19**, 3731 (2009).
- H.J. Zhang, G.H. Chen and D.W. Bahnemann, *J. Mater. Chem.*, **19**, 5089 (2009).
- T. Takata and K. Domen, *J. Phys. Chem. C*, **113**, 19386 (2009).
- G.K. Mor, K. Shankar, M. Paulose, O.K. Varghese and C.A. Grimes, *Nano Lett.*, **5**, 191 (2005).
- M. Morishita, Y. Shiraishi and T. Hirai, *J. Phys. Chem. B*, **110**, 17898 (2006).
- G. Li, D. Zhang, J.C. Yu and M.K.H. Leung, *Environ. Sci. Technol.*, **44**, 4276 (2010).
- Y. Cong, J. Zhang, F. Chen, M. Anpo and D. He, *J. Phys. Chem. C*, **111**, 10618 (2007).
- G.K. Mor, K. Shankar, M. Paulose, O.K. Varghese and C.A. Grimes, *Nano Lett.*, **6**, 215 (2006).
- A. Di Paola, E. García-López, G. Marci and L. Palmisano, *J. Hazard. Mater.*, **211**, 3 (2012).
- M. Miyauchi, A. Nakajima, T. Watanabe and K. Hashimoto, *Chem. Mater.*, **14**, 2812 (2002).
- A. Akyol and M. Bayramoglu, *J. Hazard. Mater. B*, **124**, 241 (2005).
- N. Daneshvar, D. Salari and A.R. Khataee, *J. Photochem. Photobiol. Chem.*, **162**, 317 (2004).
- R. Comparelli, E. Fanizza, M.L. Curri, P.D. Cozzoli, G. Mascio and A. Agostiano, *Appl. Catal. B*, **60**, 1 (2005).
- H.C. Yatmaz, A. Akyol and M. Bayramoglu, *Ind. Eng. Chem. Res.*, **43**, 6035 (2004).
- S. Su, S.X. Lu and W.G. Xu, *Mater. Res. Bull.*, **43**, 2172 (2008).
- A. Sharma, P. Rao, R.P. Mathur and S.C. Ameta, *J. Photochem. Photobiol. A*, **86**, 197 (1995).
- F.D. Mai, C.C. Chen, J.L. Chen and S.C. Liu, *J. Chromatogr. A*, **1189**, 355 (2008).
- B. Pare, S.B. Jonnalagadda, H. Tomar, P. Singh and V.W. Bhagwat, *Desalination*, **232**, 80 (2008).
- C. Lu, Y. Wu, F. Mai, W. Chung, C. Wu, W. Lin and C. Chen, *J. Mol. Catal. Chem.*, **310**, 159 (2009).
- G. Torres Delgado, C.I. Zúñiga Romero, S.A. Mayén Hernández, R. Castaneda Pérez and O. Zelaya Angel, *Sol. Energy Mater. Sol. Cells*, **93**, 55 (2009).
- N. Sobana and M. Swaminathan, *Sol. Energy Mater. Sol. Cells*, **91**, 727 (2007).
- S.K. Kansal, A. Hassan Ali and S. Kapoor, *Desalination*, **259**, 147 (2010).
- E. Yassitepe, H.C. Yatmaz, C. Öztürk, K. Öztürk and C. Duran, *J. Photochem. Photobiol. Chem.*, **198**, 1 (2008).
- S. Navarro, J. Fenoll, N. Vela, E. Ruiz and G. Navarro, *J. Hazard. Mater.*, **172**, 1303 (2009).
- C.C. Chen, *J. Mol. Catal. Chem.*, **264**, 82 (2007).
- C.A.K. Gouvêa, F. Wypych, S.G. Moraes, N. Durán, N. Nagata and P. Peralta-Zamora, *Chemosphere*, **40**, 433 (2000).
- A. Akyol, H.C. Yatmaz and M. Bayramoglu, *Appl. Catal. B*, **54**, 19 (2004).
- S. Sakthivel, B. Neppolian, M.V. Shankar, B. Arabindoo, M. Palanichamy and V. Murugesan, *Sol. Energy Mater. Sol. Cells*, **77**, 65 (2003).
- C. Lizama, J. Freer, J. Baeza and H.D. Mansilla, *Catal. Today*, **76**, 235 (2002).
- I. Poullos and I. Tsachpinis, *J. Chem. Technol. Biotechnol.*, **74**, 349 (1999).
- B. Neppolian, S. Sakthivel, B. Arabindoo, M. Palanichamy and V. Murugesan, *J. Environ. Sci. Health A*, **34**, 1829 (1999).
- V. Kandavelu, H. Kastien and K.R. Thampi, *Appl. Catal. B*, **48**, 101 (2004).
- P. Percherancier, R. Chapelon and B. Pouyet, *J. Photochem. Photobiol. Chem.*, **87**, 261 (1995).
- A.A. Khodja, T. Sehili, J.-F. Pilichowski and P. Boule, *J. Photochem. Photobiol. Chem.*, **141**, 231 (2001).
- I. Poullos, M. Kositz and A. Kouras, *J. Photochem. Photobiol. Chem.*, **115**, 175 (1998).
- G. Colón, M.C. Hidalgo, J.A. Navío, E. Pulido Melián, O. González Díaz and J.M. Doña Rodríguez, *Appl. Catal. B*, **83**, 30 (2008).
- M.C. Yeber, J. Rodríguez, J. Freer, J. Baeza, N. Durán and H.D. Mansilla, *Chemosphere*, **39**, 1679 (1999).
- L.B. Khalil, W.E. Mourad and M.W. Rophael, *Appl. Catal. B*, **17**, 267 (1998).
- E. Evgenidou, I. Konstantinou, K. Fytianos, I. Poullos and T. Albanis, *Catal. Today*, **124**, 156 (2007).
- A. Akyol and M. Bayramoglu, *J. Chem. Technol. Biotechnol.*, **85**, 1455 (2010).
- E. García-López, G. Marci, N. Serpone and H. Hidaka, *J. Phys. Chem. C*, **111**, 18025 (2007).
- D. Mijin, M. Savic, P. Snežana, A. Smiljanic, O. Glavaški, M. Jovanovic and S. Petrovic, *Desalination*, **249**, 286 (2009).
- A. Abdel Aal, S.A. Mahmoud and A.K. Aboul-Gheit, *Nanoscale Res. Lett.*, **4**, 627 (2009).
- S. Iijima, *Nature*, **354**, 56 (1991).
- P. Sundqvist, F.J. Garcia-Vidal, F. Flores, M. Moreno-Moreno, C. Gómez-Navarro, J.S. Bunch and J. Gómez-Herrero, *Nano Lett.*, **7**, 2568 (2007).
- Y.T. Kim, K. Ohshima, K. Higashimine, T. Uruga, M. Takata, H. Suematsu and T. Mitani, *Angew. Chem. Int. Ed.*, **45**, 407 (2006).
- M.A. Correa-Duarte, N. Sobal, L.M. Liz-Marzan and M. Giersig, *Adv. Mater.*, **16**, 2179 (2004).
- A. Gomathi, S.R.C. Vivekchand, A. Govindaraj and C.N.R. Rao, *Adv. Mater.*, **17**, 2757 (2005).
- J. Khanderi, R.C. Hoffmann, A. Gurlo and J.J. Schneider, *J. Mater. Chem.*, **19**, 5039 (2009).
- Y. Sun, S.R. Wilson and D.I. Schuster, *J. Am. Chem. Soc.*, **123**, 5348 (2001).
- Y. Yao, G. Li, S. Ciston, R.M. Lueptow and K.A. Gray, *Environ. Sci. Technol.*, **42**, 4952 (2008).
- L. Jiang and L. Gao, *Mater. Chem. Phys.*, **91**, 313 (2005).

55. A.I. Vogel, A Textbook of Quantitative Inorganic Analysis, Longmans, London, edn 4 (1978).
56. Q.-H. Yang, P.-X. Hou, S. Bai, M.-Z. Wang and H.-M. Cheng, *Chem. Phys. Lett.*, **345**, 18 (2001).
57. W. Wang, P. Serp, P. Kalck and J.L. Faria, *Appl. Catal. B*, **56**, 305 (2005).
58. C. Martinez, M. Canle L, M.I. Fernández, J.A. Santaballa and J. Faria, *Appl. Catal. B*, **102**, 563 (2011).
59. Y. Sun, S.R. Wilson and D.I. Schuster, *J. Am. Chem. Soc.*, **123**, 5348 (2001).
60. K. Chhor, J.F. Bocquet and C. Colbeau-Justin, *Mater. Chem. Phys.*, **86**, 123 (2004).
61. M. Olek, T. Busgen, M. Hilgendorff and M. Giersig, *J. Phys. Chem. B*, **110**, 12901 (2006).
62. S. Ghasemi, S. Rahimnejad, S.R. Setayesh, M. Hosseini and M.R. Gholami, *Prog. React. Kinet. Mech.*, **34**, 55 (2009).
63. B.Y. Wei, M.C. Hsu, P.G. Su, H.M. Lin, R.J. Wu and H.J. Lai, *Sens. Actuators B Chem.*, **101**, 81 (2004).
64. A.A. Ismail, I.A. Ibrahim and R.M. Mohamed, *Appl. Catal. B*, **45**, 161 (2003).
66. M.R. Hoffmann, S.T. Martin, W. Choi and D.W. Bahnemann, *Chem. Rev.*, **95**, 69 (1995).
66. J.G. Yu, X.J. Zhao and Q.N. Zhao, *Thin Solid Films*, **379**, 7 (2000).